International Journal of Infectious Diseases 80 (2019) 122–128

Contents lists available at ScienceDirect

International Journal of Infectious Diseases

journal homepage: www.elsevier.com/locate/ijid

Visual and brainstem auditory evoked potentials in HCV-infected patients before and after interferon-free therapy — A pilot study

Marta Waliszewska-Prosół[a], Joanna Bladowska[b,*], Maria Ejma[a], Katarzyna Fleischer-Stępniewska[c], Weronika Rymer[c], Marek Sąsiadek[b], Tomasz Pawłowski[d], Krzysztof Małyszczak[d], Małgorzata Inglot[c], Agnieszka Żelwetro[e], Przemysław Podgórski[b], Brygida Knysz[c]

[a] Department of Neurology, Wroclaw Medical University, Borowska 213, 50-556 Wroclaw, Poland
[b] Department of General Radiology, Interventional Radiology and Neuroradiology, Chair of Radiology, Wroclaw Medical University, Borowska 213, 50-556 Wroclaw, Poland
[c] Department of Infectious Diseases, Liver Diseases and Acquired Immune Deficiency, Wroclaw Medical University, Koszarowa 5, 51-149 Wroclaw, Poland
[d] Division of Psychotherapy and Psychosomatic Medicine, Department of Psychiatry, Wroclaw Medical University, L. Pasteura 10, 50-367 Wrocław, Poland
[e] The Institute of Psychology, University of Wroclaw, J.W. Dawida Street 1, 50-527 Wroclaw, Poland

ARTICLE INFO

Article history:
Received 30 November 2018
Received in revised form 2 January 2019
Accepted 4 January 2019
Corresponding Editor: Eskild Petersen, Aarhus, Denmark

Keywords:
HCV
Interferon-free therapy
Evoked potentials
Magnetic resonance imaging

ABSTRACT

Introduction: The aim of this study was to investigate brain bioelectrical activity disturbances in HCV-positive patients before and 24 weeks after interferon-free therapy (DAA), using visual (VEP) and brainstem (BAEP) evoked potentials and advanced magnetic resonance techniques.
Materials and methods: 11 HCV-infected patients (6 women, 5 men, mean age 51 years old) and 30 healthy controls, sex and age-matched, were studied. Clinical neurological examinations, VEP, BAEP, diffusion tensor imaging (DTI) and perfusion weighted imaging (PWI) were performed.
Results: 11 patients achieved a sustained viral response, and liver fibrosis regression in APRI and in elastography were observed. The mean P100 latency was significantly shorter in HCV-patients after therapy compared to the values before treatment ($p < 0.05$). The mean wave BAEP V latency and I–V interpeak latency were significantly longer in the HCV-infected patients before therapy compared to HCV-patients after therapy.
Conclusions: This study confirms that treatment with DAA in patients with chronic HCV infection positively affects the bioelectrical activity of the brain. An increase in the amplitude of EP after treatment indicates an improvement in the activity of the cerebral cortex. EP examination may be a useful method of assessing the function of the nervous system before and after antiviral treatment.

Introduction

Chronic infection with hepatitis C virus (HCV) is a major health problem, with more than 180 million people chronically infected (Mohd et al., 2013; Cacoub et al., 2016). Up to 70% of patients with the HCV infection experienced a variety of extrahepatic manifestations, including neurological symptoms. They may be the first sign of the disease (Cacoub et al., 2016; Mariotto et al., 2014).

Neurologic manifestations in patients with chronic HCV infection may present with non-specific general features such as fatigue, subclinical cognitive impairment, depression and neurocognitive disorders (Adinolfi et al., 2015; Köşkderelioğlu et al., 2016). These signs are unrelated to the HCV genotype or stage of liver fibrosis and to activity of hepatitis (Maisonobe et al., 2002; Kramer et al., 2002). The mechanism responsible for extrahepatic manifestations is still unknown. Results of many studies suggest that the HCV may cause brain dysfunction *per se*, while other hypotheses apply HCV-related vasculitis lesion, perivascular mononuclear inflammation and mixed cryoglobulinemia (Kramer et al., 2002; Ramos-Casals et al., 2017). The results of advanced MR techniques revealed neurotoxicity of HCV reflected by neuronal impairment within white matter, cortical hypoperfusion and

* Corresponding author at: General Radiology, Interventional Radiology and Neuroradiology, Wroclaw Medical University, Borowska 213, 50-556 Wroclaw, Poland.
E-mail address: asia.bladowska@gmail.com (J. Bladowska).

https://doi.org/10.1016/j.ijid.2019.01.011

disintegrity within several white matter tracts (Bladowska et al., 2013).

New, precise and non-invasive methods of assessment of the nervous system in patients with chronic HCV infection are sought. The study of evoked potentials (EP) is a sensitive technique that enables the evaluation of the brain's bioelectrical activity. It is particularly useful in patients with mild or no clinical symptoms of the disease. Similarly, advanced magnetic resonance (MR) techniques such as diffusion tensor imaging (DTI) and perfusion-weighted imaging (PWI) can detect even subtle cerebral changes within so-called normal appearing white and grey matter in asymptomatic patients, which are not visible via conventional MR imaging.

The new interferon (IFN) free therapies based on direct-acting antiviral agents (DAA) with an excellent efficacy and safety profile are recommended in therapy for chronic hepatitis C (Majumdar et al., 2016). There are no data available on the influence of DAAs on central nervous system function.

This study aimed to investigate brain bioelectrical activity disturbances in HCV-positive patients before and after DAA using visual and brainstem evoked potentials. The analysed EP parameters were correlated with MR imaging and hepatological data before and after DAA therapy.

We hypothesized that DAA can cause some improvement of brain bioelectrical activity in chronically HCV-infected patients.

Materials and methods

All patients gave their informed consent to participate in the study and the project was approved by the Commission of Bioethics at the Wroclaw Medical University.

The observational prospective study was carried out between January 2015 and March 2016. The study group consisted of 11 patients (6 female and 5 male; mean age 51 years, range 33–69 years) with chronic hepatitis C. HCV genotype in 8 patients was 1b, in 3 patients 1a. Drug or alcohol abuse, HIV infection and neurological disorders were excluded in the study group. All patients previously experienced, when treated with pegylated interferon alfa with ribavirin relapse, null response or breakthrough. In 5 patients advanced fibrosis or liver cirrhosis was found but in no patient was liver function decompensation observed (Table 1). HCV RNA level in nine patients was above 800 000 IU/ml (mean HCV RNA 1 710 000; 46 400–12 800 000). All patients underwent antiviral treatment with ombitasvir, paritaprevir boosted with ritonavir and dasabuvir, with or without ribavirin (OBV/PTV/r/DSV ±RBV, 3D ± RBV). Duration of the therapy varied from 12 to 24 weeks depending on HCV subgenotype and liver disease stage. The schedule was based on the guidelines of the European Association for the Study of the Liver (EASL) (EASL, 2014).

Chronic HCV infection was confirmed by HCV RNA presence for at least 6 months. HCV RNA levels were measured by PCR using the GeneProof Hepatitis C (HCV) PCR Kit (GeneProof a.s., Brno, Czech Republic). Amplification, data acquisition, and analysis were performed on a Rotor-Gene 3000 (Corbett Research, Australia). The value of 18 IU/ml was established as a lower threshold of quantification.

Liver fibrosis was measured with real-time shear wave elastography (SWE) using the Aixplorer US system (SuperSonic Imagine S.A., Aix-en-Provence, France) with a convex broadband probe (SC6-1). Liver stiffness was validated for hepatitis C (Ferraioli et al., 2012). An AST to Platelet Ratio Index (APRI) was calculated based on laboratory tests performed routinely in a local laboratory with an APRI score greater than 0.7 as a cut-off value for predicting advanced fibrosis and 1.0 as a cut-off value for cirrhosis (Lin et al., 2011).

Neurologic evaluation

All participants underwent detailed neurological examinations, MRI imaging of the head and EP studies. Patients were evaluated twice: (1) up to one month before treatment started and (2) at 24 weeks after the end of treatment.

Evoked potentials protocol

The procedure used for recording EP was compliant with the International Federation of Clinical Neurophysiology (Nuwer et al., 1994). EP were recorded using superficial electrodes placed in Fz, Cz and Pz, according to the international 10–20 system. We used superficial Ag/AgCl electrodes and their impedance was maintained below 5 kΩ (VEP) and 2 kΩ (BAEP). Each registration was done twice to assess the reproducibility of responses.

The stimulus for VEP was a chessboard pattern of black and white squares which were aired by a TV monitor from a distance of 1 m. The angular size of each square was 1.1 degrees, and the entire field of view was 18 × 22 degrees. The contrast between the black and white fields exceeds 90%. There was stimulus of both left and right eye with a frequency of 1.88 Hz. The receiving electrode was placed in the midline occipital (Oz), the reference electrode in the frontal (Fz) and with a forearm ground. The average 75 response in the frequency range 1–30 Hz at the time of analysis was 500 ms. P100 wave latency, inter-difference P100 wave latency (latency relative) and the amplitude of the complex P100/N145 were analysed.

Table 1
Clinical characteristics of HCV patients.

	Sex	Age	Before treatment					24 weeks post-treatment		
			HCV RNA	HCV GT	AIX kPa	Metavir	APRI	AIX kPa	Metavir	APRI
1	M	37	1870000	1b	6.4	1	0.33	5.8	0	0.234
2	M	34	46400	1b	21.42	4	10.98	18.62	4	2.5
3	F	37	981000	1b	12.66	4	0.545	8.6	2	0.28
4	F	54	10400000	1b	7.82	1	2.02	5.24	0	0.448
5	M	55	12800000	1b	6.98	1	0.438	5.44	0	0.309
6	M	61	943000	1b	18.78	4	4.639	9.5	2.5	0.768
7	F	62	3930000	1b	19.92	4	4.533	13.68	3.5	1.441
8	F	62	151000	1b	6	0	0.366	n/d*	n/d	0.337
9	M	34	984000	1a	7.56	1	0.793	5.8	0	0.237
10	F	66	1710000	1a	14.08	4	2.05	7.36	2	0.387
11	F	61	91500	1a	7.2	1	0.41	5.1	0	0.21
								p = 0.0055		p = 0.002

HCV GT — HCV genotype.
AIX kPa — liver stiffness measured in kPa with shear wave elastography (SWE) using the Aixplorer US system.
Metavir — fibrosis in Metavir score calculated from liver stiffness measurements with SWE n/d – not done at 24 week post -treatment.

BAEP were recorded after stimulation of right and left ear auditory stimulus (click) presented through headphones, with a duration of 0.1 ms, frequency of 20.3 Hz and an intensity of 65 dB above the individual hearing threshold. In each of the subjects, an individual hearing threshold "click" was marked. For unaudited ear intensity, a masking noise 35 dB above the hearing threshold was transmitted. Ipsilateral replies were recorded using electrodes placed on the right and left ears, with the reference electrode at the vertex (A1 or A2, relative to Cz) and with a forearm ground. They averaged 2,000 responses in the frequency range 150–3000 Hz. Analysis time was 10 ms. Analysis concerned the absolute latencies of waves I–VI; I–III, III–V, I–V interpeaks and the amplitude of waves I and V. Prolonged interpeaks to I–III and/or III–V were considered pathological only when accompanied by the prolonged latency of interpeak I–V, and the prolonged latency of wave I, when they were accompanied by changes in the latency of further components of the auditory brainstem response.

MR imaging protocols

Imaging was done on a 1.5T Signa Hdx MR unit (GE Healthcare) with a head 16-channel coil. First plain MR sequences were performed as followed: axial, sagittal, and coronal T2-weighted images, axial T1-weighted and FLAIR (fluid-attenuated inversion recovery sequence) images, as well as diffusion-weighted imaging (DWI). The protocols of advanced MR techniques such as DTI and PWI used in this study were the same as in the previously published pilot paper (Bladowska et al., 2013). Post-processing of the images was conducted using updated ReadyView software (GE Healthcare, ADW 4.6).

Diffusion tensor imaging (DTI)

DTI examinations were performed using a single shot SE EPI sequence in 25 coding directions. The parameters of the DTI study are as follows: TR 8500 ms, TE 100 ms, matrix 128 × 128, FOV 24 × 24 cm, number of excitations = 2, b values 0 and 1000 s/mm2. Axial 4 mm-thick slices with no spacing were obtained. The total acquisition time was 7 min 31 s. Post-processing of the DTI data was conducted on commercial workstations (GE Healthcare, ADW 4.6.) using ReadyView software to generate colour-coded and parametric maps of fractional anisotropy (FA) and apparent diffusion coefficient (ADC). In order to calculate FA as well as ADC values, small, circular regions of interest (ROIs) (size 30 mm2) within the selected white matter fibres under control of colour-coded maps were obtained. The assessed fourteen white matter fibres were defined using available anatomy atlases and publications (Jellison et al., 2004). FA and ADC values were measured on axial slices within selected fibre tracts. In the study commissural, association, as well as projection tracts were evaluated. The assessed commissural tracts included genu (GCC) and splenium (SCC) of the corpus callosum at the level of basal ganglia. The association fibres were as follows: inferior longitudinal fasciculi (ILFs) at the level of midbrain, inferior fronto-occipital fasciculi (IFOFs) at the level of inferior aspects of thalami laterally to the occipital horns of lateral ventricles, superior longitudinal fasciculi (SLFs) at the level of superior aspects of lateral ventricles and bilateral posterior cingulum (PC) fibres. The projection tracts comprised posterior limbs of internal capsules (PLICs) and middle cerebellar peduncles (MCPs).

Perfusion weighted imaging (PWI)

Perfusion study was done with a dynamic susceptibility contrast (DSC) method, using a gradient-recalled T2*-weighted echo-planar imaging sequence, with the following parameters: TR/TE = 1900/80 ms, flip angle = 80°, number of excitations = 1, matrix size = 192 × 128, and slice thickness = 5 mm (with no gap). Perfusion images were obtained in axial slices parallel to anterior commissure – posterior commissure (AC-PC) line. Image acquisition started 10 s before contrast agent administration in order to establish a pre-contrast baseline. Ten seconds after the beginning of image acquisition, 0.2 mmol/kg of body weight gadopentetate dimeglumine was injected, followed immediately by a bolus injection of saline (20 mL at 5 mL/s). Contrast media was injected using a power injector (Medrad) at a rate of 5 mL/s through an intravenous catheter placed in the antecubital vein. Total acquisition time was 1 min and 20 s.

Post-processing of the obtained dynamic perfusion images was performed with the ReadyView software (GE Healthcare, ADW 4.6). Cerebral blood volume (CBV) and cerebral blood flow (CBF) maps were computed on a pixel-wise basis from the first–pass data according to the study by Belliveau et al. (Belliveau et al., 1990). All rCBV and rCBF measurements were normalised to the mean values in the cerebellar cortex, which has been considered as the region minimally affected in patients with neurocognitive disorders (Talbot et al., 1994). CBV as well as CBF measurements were calculated from the following regions of interest (ROIs): placed manually in both cerebellar hemispheres (circular ROIs, size 525 mm2), frontal cortices (16 mm above AP-CP), temporoparietal cortices (8 mm above AP-CP), the posterior cingulate gyrus (PCG) region (single circular ROI, size 525 mm^2), the basal ganglia regions (irregular hand-drawn ROIs outlining the putamen, globus pallidus and caudate nucleus, size 500–600 mm^2) as well as frontoparietal white matter in the centrum semiovale (circular ROIs, size 525 mm^2). Temporoparietal and frontal ROIs were almost rectangular in shape (size 800- 1000 mm^2).

The control group (CG)

The healthy age- and sex-matched control group consisted of 30 subjects, mainly hospital staff (15 women and 15 men; mean age 50 years, range 34–68) with excluded HCV infection (negative result of anti-HCV antibodies), no history of liver disease, drug abuse, or neurological disorders. They did not suffer from concurrent diseases that could have affected the brain's electrical activity.

Statistical analysis

Data analysis was performed with Statistica v.13 software. Median, IQR and range were reported. The two-tailed Wilcoxon's test (for dependent variables) and Mann-Whitney U test (for independent variables) were used. P values <0.05 were considered significant. The mean range of ± 2 SD was assumed as the range of correct values of individual BAEP and VEP components. Over 50% of the amplitude of the P100/N145 complex of the left and the right eye was recognised as pathological, and the difference of I and V waves obtained during left and right ear stimulation was over 50%.

Results

The neurological examination before and after therapy was normal in all patients. All patients achieved a sustained viral response measured as undetectable HCV RNA at 24 weeks after treatment. The parameters of liver fibrosis measured as liver stiffness and APRI improved (Table 1).

Evoked potentials

Abnormal VEP and BAEP before therapy were recorded in 45% of the patients. In 2 patients there were prolonged latencies P100 VEP,

in 3 patients there were prolonged V latency and I–V interpeak latency of BAEP. After therapy abnormal EPs were recorded in 2 patients (1–VEP, 1–BAEP) (Figure 1, Figure 2). The same patients had abnormal potentials before and after treatment.

The mean P100 and N145 VEP latencies were significantly longer in the HCV-infected patients before and after therapy compared to the control group ($p < 0.0001$ vs $p = 0.004$). The mean P100 latency was significantly shorter in HCV-patients after therapy compared to the values before treatment ($p < 0.05$) (Table 2).

The mean wave BAEP V latency and I–V interpeak latency were significantly longer in the HCV-infected patients before therapy compared to HCV-patients after therapy (Table 2).

Significant correlation between fractional anisotropy (FA) and VEP and BAEP parameters in HCV-infected patients after treatment were recorded in seven locations: right and left middle cerebellar peduncle, right interior longitudinal fascicules, left interior fronto-occipital fascicules, genu of the corpus callosum, posterior limb of left internal capsule and right posterior cingulum fibres (Table 3, Table 4).

The ADC values did not significantly correlate with VEP and BAEP parameters.

There were no statistically significant correlations between the mean VEP and BAEP parameters and liver stiffness, the stage of liver fibrosis and activity of hepatitis.

Discussion

Our study attempts to assess brain bioelectrical activity in patients with chronic HCV infection before and after DAA treatment using a very sensitive method called evoked potential technique. To the best of our knowledge, this is the first study concerning VEP and BAEP in HCV-infected patients after DAA therapy.

The involvement of the optic nerve in the course of HCV infection is rare. The most frequently reported complications concern iatrogenic subacute neuropathy and transient visual loss associated with pegylated interferon treatment (Jancoriene et al., 2014). Case reports refer to the severe course of neuromyelitis optica or NMOSD (neuromyelitis optica spectrum disorders) in patients with chronic HCV (Mariotto et al., 2014; Obara et al., 2018). The authors of the cases suggest that HCV infection may additionally activate the production of antibodies to AQP4 by autoreactive B-lymphocytes and thus contribute to the development of NMO (Mariotto et al., 2014). The literature also discusses the direct impact of the virus on demyelination of the optic nerves and peripheral nerves resulting in frequent coexistence in patients with HCV diseases such as: CIDP (chronic inflammatory demyelinating polyneuropathy), AIDP (acute inflammatory demyelinating polyneuropathy), or Miller-Fisher syndrome (Mariotto et al., 2014; De Klippel et al., 1993).

Köşkderelioğlu et al. analysed VEP in 30 HCV-infected patients without other burden. They showed a significantly lower P100 wave amplitude in the group of patients compared to the control group, and did not find statistically significant differences in latencies between these groups. The same authors also compared VEP in patients treated and untreated with interferon, not finding statistically significant differences in VEP parameters in both groups (Köşkderelioğlu et al., 2016). In other individual reports, the effect of interferon treatment on the prolongation of P100 latency was demonstrated (Moschos et al., 1998; Manesis et al., 1998). All patients in our study group were treated with interferon in the past (more than 12 months before the study). Our study showed significantly longer latency of P100 and N145 waves in patients with HCV both before ($p < 0.0001$) and after treatment ($p = 0.004$) DAA in comparison to the control group. We showed that before treatment, the P100 wave latency was significantly longer than after treatment, which indicates improved visual conduction velocity. This may be related to the regeneration of nerve fibres within the optic nerve.

Hearing disorders in HCV-infected patients, as well as visual disturbances, are most often related to the treatment used. A complication quite often described in the literature is a sudden sensorineural hearing loss most often associated with treatment with pegylated interferon (Wong et al., 2005). The precise etiology of this disorder consisting in a sudden decrease in hearing acuity of approximately 30 dB is still unknown. Vascular, immunisation or infectious background is being considered (Chen et al., 2017). The impact of HCV infection on the functionality of the auditory path was not analysed, and the incidence of otolaryngological complications unrelated to treatment in these patients is unknown. In the available literature, only one BAEP analysis can be found in patients with HCV. Cappellari et al. (Cappellari et al., 2006) found in 4 of 18 (22%) patients with HCV-related mixed cryoglobulinemia abnormal BAEP. Nai-Shin Chu et al. analysed BAEP in 69 patients with

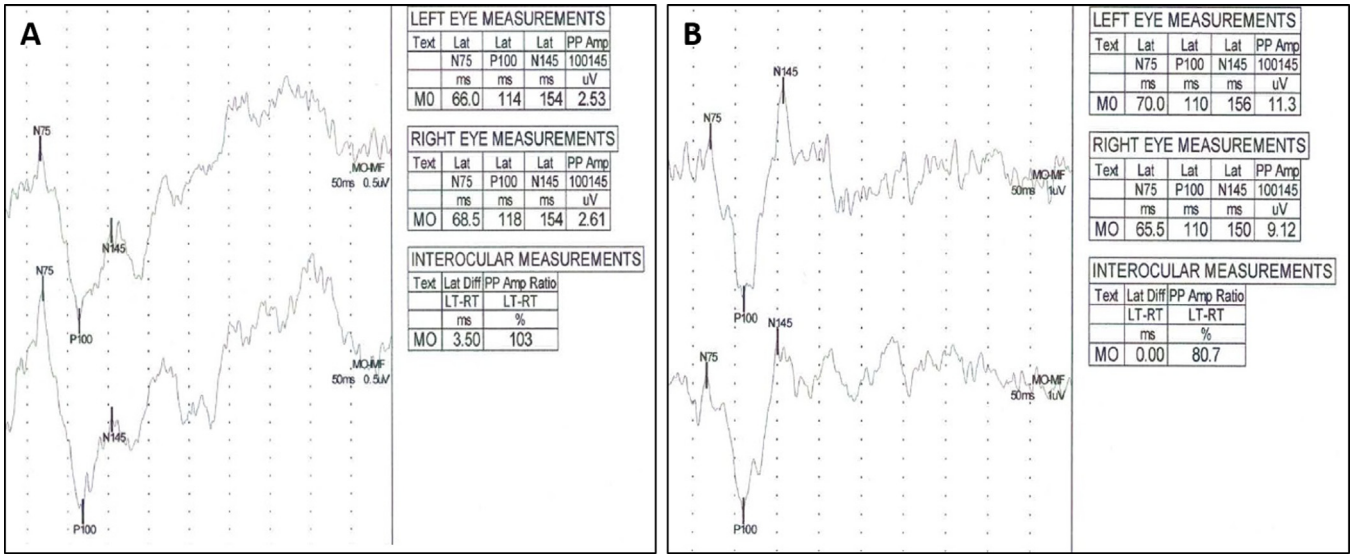

Figure 1. VEP in HCV-infected male before (A) and after interferon-free therapy (B). Prolonged latencies P100 (L–114 ms, R–118 ms) (A). Normal P100 latencies (L–110 ms, R–110 ms) (B).

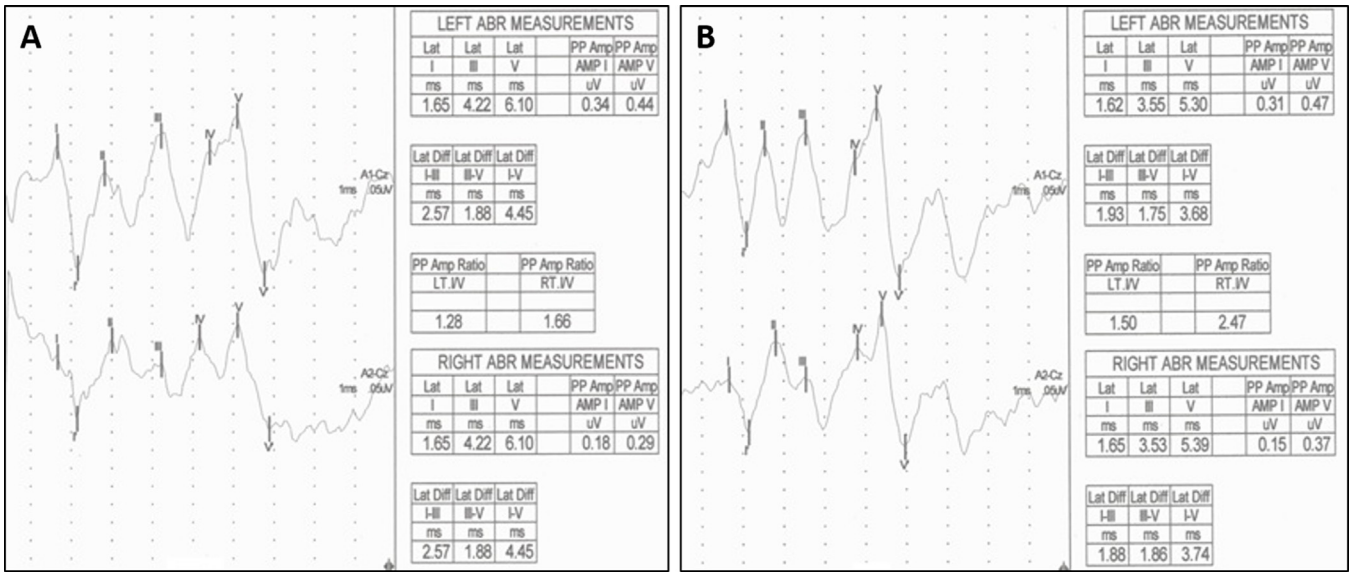

Figure 2. BAEP in HCV-infected female before (A) and after interferon-free therapy (B). Prolonged latencies and interpeak latencies: V (L-6.10 ms, R-6.10 ms), and I–V (L-4.45 ms, R-4.45 ms) (A). Normal latencies and interpeak latencies: V (L-5.30 ms, R-5.39 ms), and I–V (L-3.68 ms, R-3.74 ms) (B).

Table 2
Median values of EP parameters in HCV-infected patients before treatment (HCV1), after treatment (HCV2) and the control group (CG) with the results of the Wilcoxon's test (HCV1 vs HCV2) and the Mann–Whitney U test (HCV1 and HCV2 vs CG).

VEP	Median + SD			p Values		
	HCV1	HCV2	CG	HCV1 vs HCV2	HCV1 vs CG	HCV2 vs CG
Latency (ms)						
N75	70.87 ± 2.6	69.77 ± 2.71	70.19 ± 6.67	0.202	0.679	0.792
P100	108.03 ± 4.31	105.29 ± 4.15	101.72 ± 3.2	**0.010***	**<0.0001***	**0.004***
N145	155.25 ± 8.07	152.15 ± 6.79	144.05 ± 8.6	0.196	**<0.0001***	**0.002***
Amplitude P100/N145 (mV)	7.73 ± 3.96	8.68 ± 3.84	9.42 ± 2.79	0.446	0.128	0.49
BAEP						
Latency (ms)						
I	1.72 ± 0.14	1.70 ± 0.17	1.65 ± 0.10	0.897	0.116	0.213
III	3.84 ± 0.13	3.77 ± 0.16	3.79 ± 0.17	0.149	0.345	0.656
V	5.83 ± 0.24	5.67 ± 0.24	5.63 ± 0.20	**0.041***	**0.001***	0.587
I-III	2.12 ± 0.16	2.06 ± 0.17	2.14 ± 0.13	0.232	0.745	0.124
III-V	1.98 ± 0.19	1.94 ± 0.18	1.83 ± 0.19	0.490	**0.001***	0.145
I-V	4.12 ± 0.2	3.99 ± 0.18	3.98 ± 0.19	**0.042***	**0.04***	0.847
Amplitude (mV)						
I	0.17 ± 0.09	0.28 ± 0.13	0.33 ± 0.10	**0.003***	**<0.0001***	0.173
V	0.39 ± 0.11	0.42 ± 0.12	0.49 ± 0.17	0.371	**0.001***	0.190
I/V	3.03 ± 1.92	2.08 ± 1.14	1.45 ± 0.48	0.06	**<0.0001***	0.100

* — statistically significant changes ($p < 0.05$).

Table 3
Significant correlation between fractional anisotropy (FA) and VEP parameters in HCV-infected patients after treatment.

FA and VEP parameters after treatment	p Values	R-Spearman	t(N-2)
ROI 1 vs. latency N145	0.003	−0.66	−2.5
ROI 2 vs. amplitude P100/N145	0.001	0.86	4.91
ROI 3 vs latency N145	**0.03**	**−0.65**	**−2.46**
ROI 6 vs. amplitude P100/N145	0.01	0.74	3.16
ROI 7 vs. amplitude P100/N145	0.001	0.72	2.94
ROI 10 vz. latency P100	**0.005**	**−0.79**	**−3.6**
ROI 13 vs. amplitude P100/N145	0.02	0.68	2.65

*— ROI 1–right middle cerebellar peduncle, RO1 2–left middle cerebellar peduncle, ROI 3–right interior longitudinal fascicules, ROI 6–left interior fronto-occipital fascicules, ROI 7–genu of the corpus callosum, ROI 10–posterior limb of left internal capsule, ROI 13–right posterior cingulum.

liver disorders of various etiology. They showed normal results in patients with hepatitis; prolongated V-wave latencies and I–V interlatencies showed only in patients with alcoholic liver cirrhosis and Wilson's disease (Nai-Shin and Sien-Sing, 1987).

In our patients before treatment, we found significantly longer V-wave latency, III–V and I–V interlatencies, and lower amplitude of I and V-waves compared to the control group. We also found a significant shortening of V-wave latency and I–V wave intervening after DAA treatment. These results indicate improved conduction velocity within the auditory pathway.

Imaging studies also showed an increase in the integrity index of white matter after treatment. The distribution of these microstructural changes was not even, however, it included both mating and pyramidal ways as well as the branches of the cerebellum.

Our results of significant correlations between VEP and BAEP parameters and FA values in HCV-infected patients after treatment suggest that DAA therapy may lead to an improvement in brain bioelectrical activity as well as to white matter tracts recovery, including corpus callosum and cingulum fibres.

The corpus callosum plays a very important role in interhemispheric relay and integration, providing connections with multiple subcortical structures, such as the basal ganglia. It has been

Table 4
Significant correlation between fractional anisotropy (FA) and BAEP parameters in HCV-infected patients after treatment.

FA and BAEP parameters BAEP after treatment	p Values	R-Spearman	t(N-2)
ROI 10 vs. latency V	**0.04**	**−0.63**	**−2.31**
ROI 13 vs. amplitude I	0.01	0.64	2.40
ROI 13 vs. amplitude V	0.01	0.69	2.74

*— ROI 10–posterior limb of left internal capsule, ROI 13–right posterior cingulum.

reported that FA values measured in the corpus callosum may be sensitive markers of subtle and early alterations not visible on conventional MR images in the course of other CNS diseases presenting with cognitive decline (Bladowska et al., 2014).

The posterior cingulate cortex is one of the most metabolically active areas of the brain, which among others is involved in the processes of emotion and memory, as well as the control of visual attention (Leech and Sharp, 2014; Engelmann et al., 2009; Chow et al., 2018).

Furthermore, the cingulum fibres are involved in memory and learning processes which are impaired in patients with dementia syndromes (Bladowska et al., 2014; Nesteruk et al., 2016). Many published reports have indicated that the posterior cingulate region may be the strategic area which is impaired in dementia and predementia patients. MR changes found in this part of the brain are believed to be predictors of cognitive decline in presymptomatic subjects, assuming that the pathologic process starts well before even mild dementia symptoms can be diagnosed clinically (Bladowska et al., 2014; Nesteruk et al., 2016).

The significant correlations between VEP parameters and FA values in HCV subjects after therapy were observed also in both middle cerebellar peduncles. It should be stressed that the cerebellum is a unique part of the brain, which is involved not only in motor function and coordination but also in emotion (Re et al., 2016). Changes in the cerebellum may be responsible for impairment of executive function, visuo-spatial abilities, expressive language, and affective behaviour. Analysis of the fractional anisotropy measured in the cerebellar peduncles showed FA correlation with the ability to read (Travis et al., 2015). The middle cerebellar peduncle pathway runs from the cerebellum to the pons and contains two distinct subpathways: one is predominantly associated with higher cognitive function, and the other is predominantly associated with motor-sensory function (Re et al., 2016).

The limitation

The main limitation of our study is the small number of patients involved in the project. However, it should be pointed out that in the recently published paper by Kleefeld et al. only 8 HCV-positive subjects were included in the study (Kleefeld et al., 2018). Nevertheless, it is worth underlining that our report is the first study in the available literature showing results of VEP and BAEP changes in HCV-infected patients after DAA treatment.

Conclusions

Our observations confirm the fact that treatment with DAA in patients with chronic HCV infection positively affects the bioelectrical activity of the brain. The results of the correlation of EP parameters with the imaging parameters obtained by us suggest that the functional improvement demonstrated in the potentials studies may have a positive relationship/effect on the activity of certain brain regions in this cingulate cortex, which is important, e.g., for cognitive functioning. An increase in the amplitude of EP after treatment indicates an improvement in the activity of the cerebral cortex. Further studies, including larger groups of patients treated with other DAAs, are required to evaluate the significance of our discovery.

Financial Disclosures

The authors have 347 no financial relationships relevant to this article to disclose and they have no conflict of interest.

Conflict of Interest

Author's (Marta Waliszewska-Prosół, Joanna Bladowska, Maria Ejma, Katarzyna Fleischer-Stępniewska, Weronika Rymer, Marek Sąsiadek, Tomasz Pawłowski, Krzysztof Małyszczak, Małgorzata Inglot, Agnieszka Żelwetro, Przemysław Podgórski, Brygida Knysz) declares that he/she has no conflict of interest.

Ethical approval

All procedures performed in studies involving human participants were in accordance with the ethical standards of the institutional and/or national research committee and with the 1964 Helsinki declaration and its later amendments or comparable ethical standards. This article does not contain any studies with animals performed by any of the authors.

Informed consent

Informed consent was obtained from all individual participants included in the study.

References

Adinolfi LE, Nevola R, Lus G, Restivo L, Guerrera B, Romano C, et al. Chronic hepatitis C virus infection and neurological and psychiatric disorders: an overview. World J Gastroenterol 2015;21(8):2269–80.
Belliveau JW, Rosen BR, Kantor HL, Rzedzian RR, Kennedy DN, McKinstry RC, et al. Functional cerebral imaging by susceptibility-contrast NMR. Magn Reson Med 1990;14(3):538–46.
Bladowska J, Zak T, Zimny A, Zacharzewska-Gondek A, Gondek TM, Szewczyk P, et al. Assessment of metabolic changes within normal appearing gray and white matter in children with growth hormone deficiency: magnetic resonance spectroscopy and hormonal correlation. Brain Dev 2014;36:770–7.
Bladowska J, Zimny A, Knysz B, Małyszczak K, Kołtowska A, Szewczyk P, et al. Evaluation of early cerebral metabolic, perfusion and microstructural changes in HCV-positive patients: a pilot study. J Hepatol 2013;59:651–7.
Cacoub P, Comarmond C, Domont F, Savey L, Desbois AC, Saadoun D. Extrahepatic manifestations of chronic hepatitis C virus infection. Ther Adv Infect Dis 2016;3(1):3–14.
Cappellari A, Origgi L, Spina MF, Yiannopoulou KG, Meola G, Vanoli M, et al. Central nervous system involvement in HCV-related mixed cryoglobulinemia. Electromyogr Clin Neurophysiol 2006;46(3):149–58.
Chen HC, Chung CH, Wang CH, Lin J, Chang W, Lin F, et al. Increased risk of sudden sensorineural hearing loss in patients with hepatitis virus infection. PLoS One 2017;6(12)e0175266.
Chow Y, Masiak J, Mikołajewska E, Mikołajewski D, Wójcik GM, Wallace B, et al. Limbic brain structures and burnout-a systematic review. Adv Med Sci 2018;63(1):192–8.
De Klippel N, Hautekeete ML, De Keyser J, Ebinger G. Guillain-Barré syndrome as the presenting manifestation of hepatitis C infection. Neurology 1993;43(10):2143.
Engelmann JB, Damaraju E, Padmala S, Pessoa L. Combined effects of attention and motivation on visual task performance: transient and sustained motivational effects. Front Hum Neurosci 2009;3:4.
European Association for Study of Liver. EASL Clinical Practice Guidelines: management of hepatitis C virus infection. J Hepatol 2014;60(2):392–420.

Ferraioli G, Tinelli C, Dal Bello B, Zicchetti M, Filice G, Filice C. Accuracy of real-time shear wave elastography for assessing liver fibrosis in chronic hepatitis C:a pilot study. Hepatology 2012;56(6):2125–33.
Jancoriene L, Norvydaite D, Galgauskas S, Balciunaite E. Transient visual loss in a hepatitis C patient treated with pegylated interferon alfa-2a and ribavirin. Hepat Mon 2014;14(2)e15124.
Jellison BJ, Field AS, Medow J, Lazar M, Salamat MS, Alexander AL. Diffusion tensor imaging of cerebral white matter: a pictorial review of physics, fiber tract anatomy, and tumor imaging patterns. AJNR Am J Neuroradiol 2004;25(3):356–69.
Kleefeld F, Heller S, Ingiliz P, Jessen H, Petersen A, Kopp U, et al. Interferon-free therapy in hepatitis C virus (HCV) monoinfected and HCV/HIV coinfected patients: effect on cognitive function, fatigue, and mental health. J Neurovirol 2018;(May).
Köşkderelioğlu A, Ortan P, Ari A, Gedizlioğlu M. Screening for electrophysiological abnormalities in chronic hepatitis C infection: peripheral neuropathy and optic neuropathy. Noro Psikiyatr Ars 2016;53(1):23–7.
Kramer L, Bauer E, Funk G, Hofer H, Jessner W, Steindl-Munda P, et al. Subclinical impairment of brain function in chronic hepatitis C infection. J Hepatol 2002;37(3):349–54.
Leech R, Sharp DJ. The role of the posterior cingulate cortex in cognition and disease. Brain 2014;137:12–32.
Lin ZH, Xin Y, Dong Q, Wang Q, Jiang XJ, Zhan SH, et al. Performance of the aspartate aminotransferase-to-platelet ratio index for the staging of hepatitis C-related fibrosis: an updated meta-analysis. Hepatology 2011;53:726–36.
Maisonobe T, Leger JM, Musset L, Cacoub P. Neurological manifestations in cryoglobulinemia. Rev Neurol (Paris) 2002;158:920–4.
Majumdar A, Kitson M, Roberts S. Systemic review: current concepts and challenges for the direct-acting antiviral era in hepatitis C cirrhosis. Aliment Pharmacol Ther 2016;43:1276–92.
Manesis EK, Moschos M, Brouzas D, Kotsiras J, Petrou C, Theodosiadis G, et al. Neurovisual impairment: a frequent complication of alpha-interferon treatment in chronic viral hepatitis. Hepatology 1998;27(5):1421–7.
Mariotto S, Ferrari S, Monaco S. HCV-related central and peripheral nervous system demyelinating disorders. Inflamm Allergy Drug Targets 2014;13(5):299–304.
Mohd H, Hanafiah K, Groeger J, Flaxman A, Wiersma S. Global epidemiology of hepatitis C virus infection: new estimates of age-specific antibody to HCV seroprevalence. Hepatology 2013;57:1333–42.
Moschos M, Manesis E, Panagakis E, Brouzas D, Hadziyannis S, Theodossiadis G. The effect of low-dose interferon treatment on visual evoked potentials. Doc Ophthalmol 1998;94(3):215–21.
Nai-Shin CH, Sien-Sing Y. Brain-stem auditory evoked potentials in different types of hepatic diseases. Electroencephalogr Clin Neurophysiol 1987;67(4):337–9.
Nesteruk T, Nesteruk M, Styczyńska M, Barcikowska-Kotowicz M, Walecki J. Radiological evaluation of strategic structures in patients with mild cognitive impairment and early Alzheimer's disease. Pol J Radiol 2016;81:288–94.
Nuwer M, Aminoff M, Goodin D. IFCN recommended standards for brain-stem auditory evoked potentials. Report of an IFCN committee. Electroencephalogr Clin Neurophysiol 1994;91:12–7.
Obara K, Waliszewska-Prosół M, Budrewicz S, Szewczyk P, Ejma M. Severe course of neuromyelitis optica in a female patient with chronic C hepatitis. Neurol Neurochir Pol 2018;52(3):397–400.
Ramos-Casals M, Zignego A, Ferri C, Brito-Zerón P, Retamozo S, Casato M. Evidence-based recommendations on the management of extrahepatic manifestations of chronic hepatitis C virus infection. J Hepatol 2017;66(6):1282–99.
Re T, Levman J, Lim A, Righini A, Grant P, Takahashi E. High-angular resolution diffusion imaging tractography of cerebellar pathways from newborns to young adults. Brain Behav 2016;7(1)e00589.
Talbot PR, Lloyd JJ, Snowden JS, Neary D, Testa HJ. Choice of reference region in the quantification of single-photon emission tomography in primary degenerative dementia. Eur J Nucl Med 1994;21:503–8.
Travis K, Leitner Y, Feldman H, Ben-Shachar M. Cerebellar white matter pathways are associated with reading skills in children and adolescents. Hum Brain Mapp 2015;36(4):1536–53.
Wong VK, Cheong-Lee C, Ford JA, Yoshida EM. Acute sensorineural hearing loss associated with peginterferon and ribavirin combination therapy during hepatitis C treatment: outcome after resumption of therapy. World J Gastroenterol 2005;11(34):5392–3.